JOURNAL OF ENDODONTICS
Printed in U.S.A.
VOL. 27, NO. 8, AUGUST 2001

Influence of Structure on Nickel-Titanium Endodontic Instruments Failure

Grégoire Kuhn, Bruno Tavernier, and Laurence Jordan

The purpose of this work was to investigate the process history on fracture life of nickel-titanium endodontics files. The results are based on microstructural investigations of nickel-titanium engine-driven rotary instruments based on X-ray diffraction, scanning electron microscopy, and microhardness tests. Endodontic files are very work-hardened, and there is a high density of defects in the alloy that can disturb the phase transformation. The microhardness Vickers confirmed these observations (dislocations and precipitates). The X-rays show that experimental spectrum lines are extended, typical of a distorted lattice. The surface state of the endodontic files (scanning electron microscopy) is an important factor in failure and fracture initiation.

Nickel-titanium (NiTi) endodontic instruments were introduced to facilitate instrumentation of curved canals. Ni-Ti instruments are superelastic and will flex far more than stainless-steel instruments before exceeding their elastic limit (1, 2). Despite this increased flexibility many investigators have reported unexpected fractures (3). The fractures of the files can seriously jeopardize the therapy.

Difficult endodontic treatments are related to abruptness of canal curvature. The risk with traditional files is plastic deformation and fracture due to stress and strain in the canals.

Shape memory alloys (SMAs) are characterized by a thermoelastic martensitic transformation. The transformation is reversible, accompanied by a hysteresis, and can be induced by variation of either temperature or stress (4). In the case of temperature-induced martensitic transformation the formation of the martensitic phase starts at temperature Ms (Martensite Start) and ends at temperature Mf (Martensite Finish) (Fig. 1). The reversible transformation occurs between temperatures frequently noted as As (Austenite Start) and Af (Austenite Finish).

In the case of stress-induced martensitic transformation the process is driven by superelasticity; this effect is linked to structural changes at certain temperatures (Fig. 2). Austenite is transformed to martensite during loading and reverts back to austenite when unloaded. At the beginning of the strain the alloy is fully austenitic (Fig. 2*a*), at a particular stress (σp) that depends on temperature, the martensitic transformation is observed (martensite is stable with stress). The plateau has been explained as being caused by orientation of the

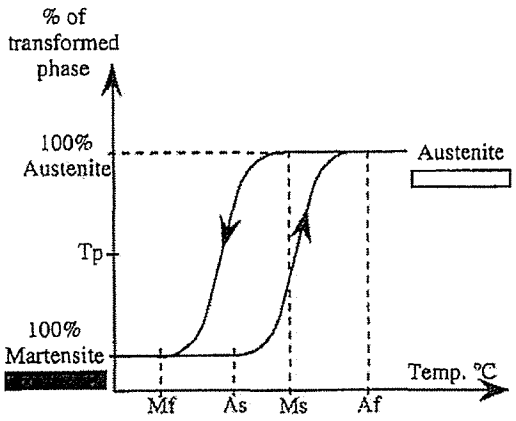

FIG 1. Theoretical thermogram of martensitic transformation temperatures. For example at Tp, two phases are present: 50% austenite + 50% martensite. *Mf*, Martensite Finish; *As*, Austenite Start; *Ms*, Martensite Start; *Af*, Austenite Finish; *Tp*, theoretical point.

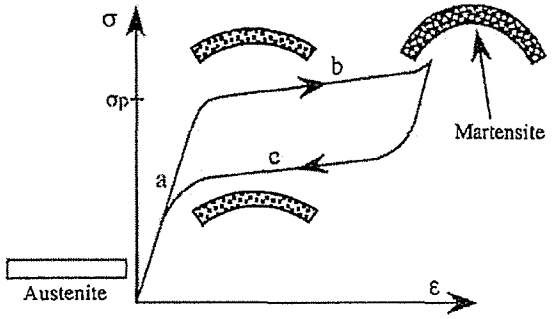

FIG 2. Schematic stress-strain curve of superelasticity; σ = stress; σp = particular stress; ε = strain.

martensite variants along the direction of the strain (Fig. 2*b*), the "easy deformation" is a consequence of a stress-induced phase transformation. Without acting strain (curvature of the root canal) or stress the martensite is unstable at root canal temperature, and specimens recover their original shape after unloading (Fig. 2*c*) (4). If austenite is not present a transformation cannot take place (superelasticity behavior does not exist).

Austenite and martensite have somewhat different atomic arrangements known as crystallographic structures (5). The crystallographic

structure of austenite is cubic, whereas that of martensite is more complex (monoclinic). X-ray diffraction (XRD) is a valuable tool for the determination of the crystallographic structure of materials. Planes (hkl) of atoms constructively interfere with X-rays and diffraction occurs: Bragg's law, $\lambda = 2d \sin\theta$, allows the calculation of interplanar spacings or d-spacings from the angular location of XRD peaks, θ (degree). Comparison of XRD date to known standards is used to identify phases. Miller indices, hkl integers, are assigned to XRD peaks. Miller indices describe the orientation of planes of atoms to the unit cell of a material's crystal structure (6).

Some authors, Miyazaki et al. (7), found superelasticity to be greatly dependent on the thermal history of the material. They showed various heat treatments can produce or eliminate superelasticity behavior. Thermal treatments are involved in promoting some systemic changes in the mechanical properties and transformation characteristics. When the metal is heated up thermally activated diffusion and partial annihilation of lattice defects will occur and the stored energy will be released in the form of heat (recovery). For the recrystallization process a different mechanism starts to operate (i.e. grain growth) with healing of defects (8).

The aim of the present work was to investigate fatigue characteristics of superelastic NiTi and subsequently the process history of fracture life.

MATERIALS AND METHODS

The engine-driven rotary instruments that were studied are produced by Maillefer (ProFile) and Micro-Mega (Hero) in many geometrical shapes. The studied files had a 25 mm length, a taper ranging between 0.04 and 0.06 mm per mm length, and sizes 20 to 40, representing the diameter of the tip base of the file given in hundredths of a millimeter.

Thermal Treatments

Different thermal treatments were investigated. The heat treatments consisted of an annealing at 350, 400, 450, 510, 600, and 700 degrees Celsius in salt baths for 10 min, and at 600° and 700°C for 15 min with the same process, and subsequent water quench.

Methodologies

Results are based on microstructural investigations of NiTi engine-driven rotary instruments with scanning electron microscopy (SEM), XRD, and microhardness.

Microhardness

For mechanical characterization the microhardness Vickers was measured with a weight less than 1.96 N. These tests were conducted at room temperature and only on the inactive part of the file (without machining). Microhardness characterizes penetration resistance of a material. Because the number of samples was small (10) the analysis of the results was performed with a Kruskal-Wallis test.

SEM

Size 20 Hero and Profile 0.04 and 0.06 tapers were observed by SEM to study the surface states. A JEOL T330 was used, and EDS analysis was performed on a Tracor TN 5500.

XRD

A Philips diffractometer was used to detect the phase present at room temperature. The wavelength of the CuKα radiation used in this study was 0.154051 nm.

RESULTS

XRD

Results of XRD of Hero and Profile files showed that the alloys are fully austenite at room temperature. The four principal peaks indicate the existence of an austenitic phase. Table 1 shows characteristic (hkl) planes of this phase.

The XRD scans of all specimens show a (110) texture. Peak width is an indication of cold work. Narrow peaks indicate easy cold work; wide ones, hard cold work.

From an enlargement of the peak (110) (Fig. 3) it is apparent that the experimental spectrum lines are extended; this shows that the lattice has been distorted and therefore that the alloys are work-hardened (9).

Microhardness

This test compared data relating to each instrument and shows a statistically significant difference among these instruments ($p < 0.005$).

Table 2 shows the average value for each instrument.

For size 20 Hero 0.06 taper and size 20 Profile 0.06 taper there was no statistically significant difference ($p = 0.0179$). After

TABLE 1. X-ray data of Hero and Profile at room temperature

θ (deg) Hero	θ (deg) Profile	Planes (hkl)	Structure
21.1682	21.1682	(110)	Austenite
38.7098	38.7736	(211)	Austenite
46.3636	46.3017	(220)	Austenite
53.9729	53.9651	(310)	Austenite

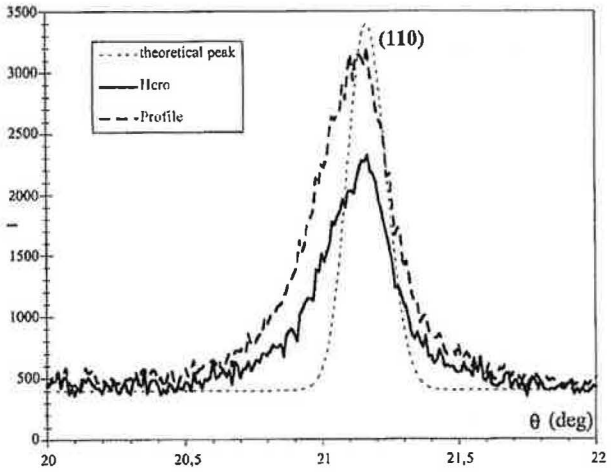

FIG 3. XRD (110) of the austenite phase for two endodontic files. A notable difference between scans of NiTi files and theoretical peak is the width of the (110) peak.

TABLE 2. Microhardness results

Endodontics Files	Average (HV)
Hero 6 20	421
Profile 6 20	475.2
Profile 4 20–350°C 10′	407.2
Profile 4 20–400°C 10′	420
Profile 4 20–450°C 10′	401.6
Profile 4 20–510°C 10′	372.4
Profile 4 20–600°C 10′	258
Profile 4 20–600°C 15′	258
Profile 4 20–700°C 10′	254.4
Profile 4 20–700°C 15′	254.2

HV, Hardness Vickers. Prime indicates minutes.

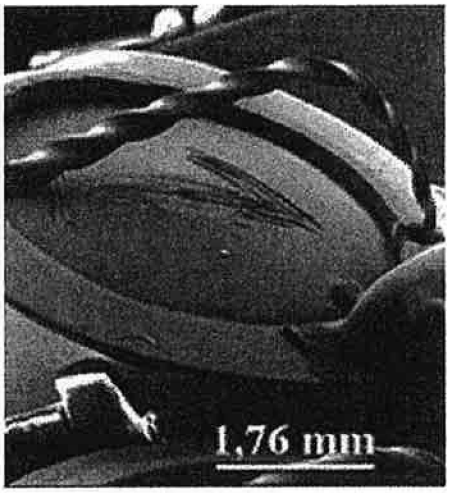

FIG 4. Presentation of the system that maintains files curved for SEM examination.

comparison of two types of heat treatments (superior to 550°C and inferior to 550°C), no significant difference was found with each type but there is a statistical difference among each group ($p = 0.0001$). Another difference appears between size 20 Profile 0.06 taper and size 20 Profile 0.04 taper that had heat treatments inferior to 550°C ($p = 0.0013$).

Our samples, before any use, were measured at a hardness above 400 HV. These samples are already work-hardened, probably with precipitates. The samples annealed at temperature below 600°C had a lesser density of defects (dislocations). For temperatures above 600°C the alloy will recrystallize and the precipitates will partially disappear.

SEM

For SEM examination the endodontic files, selected before any use, were maintained curved to generate stress-strain on the most curved part of the file (Fig. 4). SEM microphotographs of the noncurved body regions show for size 20 Profile 0.06 taper significant machining marks along the faces of the flutes (Fig. 5). For the curved body region of size 20 Profile 0.06 taper the cutting edges and ridges show irregularities and cracks. These cracks are easily identifiable because of the curvature of the instrument (Fig. 6). At this higher magnification (Fig. 7), on the top of the curvature, real sinuous-shape cracks appear.

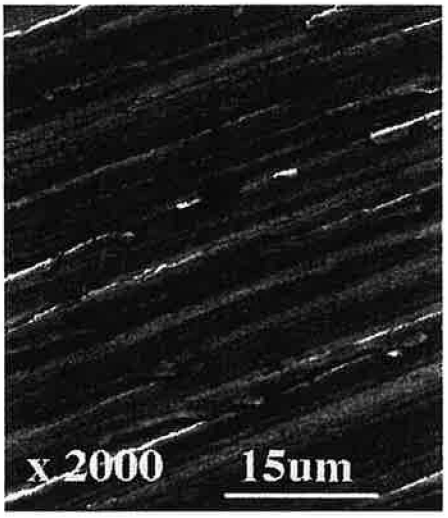

FIG 5. A size 20 Profile 0.06 taper, noncurved body region that shows striation patterns resulting from machining.

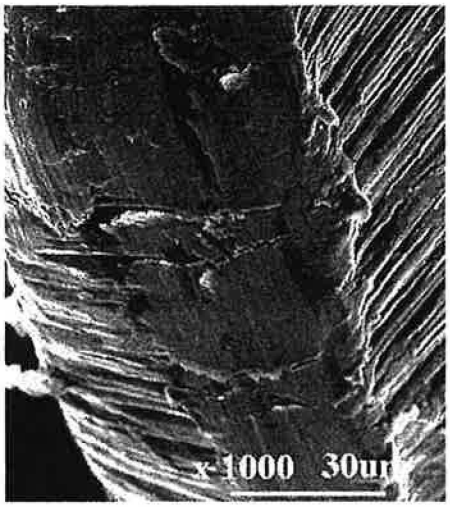

FIG 6. A size 20 Profile 0.06 taper, maximum curved area, at less magnification (×1000). The cracks are still easy identifiable when the file is under stress.

For size 20 Hero 0.06 taper SEM shows less machining damage. In deep flutes, we can observe some beginning cracks (Fig. 8), which seem to be becoming bigger near the most curved part (Fig. 9).

DISCUSSION

Some authors (10) studied the mechanical fatigue of NiTi alloys. Fatigue crack growth rates were measured and found to be lower than predicted from the phenomenological law relating growth rates to the elastic modulus. By comparison a deviation of factor 3 is observed with conventional metals or alloys (Ti-, Al-, and Fe-based alloys). This decrease in normalized crack growth rate may be a consequence of reversible martensitic deformation processes (superelasticity) leading to less accumulation of damage per cycle compared with more conventional materials.

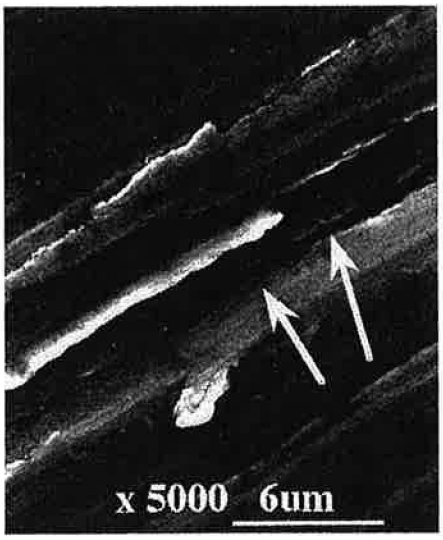

FIG 7. A size 20 Profile 0.06 taper, at a higher magnification (×5000). Real sinuous shape cracks appear (*arrows*), which mean beginning risks of fracture.

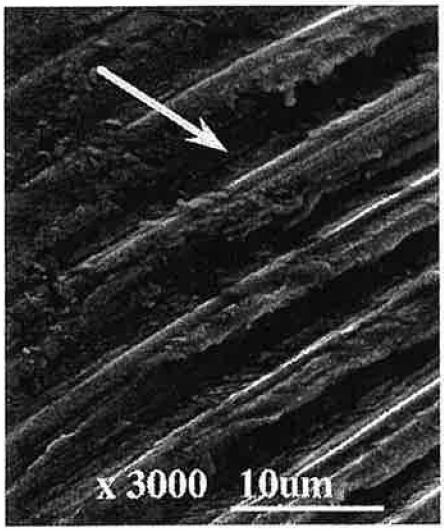

FIG 8. A size 20 Hero 0.06 taper, noncurved area. Cracks are also present (*arrow*) between every striation.

But users and the literature report "premature" failures. Moreover manufacturer's advise not to use each file on more than 10 to 12 root canals.

The purpose of the present paper was therefore to explain why these endodontic instruments are prematurely broken and the process history of fracture life.

The mechanical properties and the various phase transformation temperatures of NiTi SMAs are known to be very dependent on thermomechanical processing. When the material is subjected to deformation or stress by machining a high density of lattice defects is produced as dislocations. XRD and the microhardness Vickers results show that alloys are very work-hardened, thus the density of dislocations is very important. After Treppmann (11) a sample of NiTi fully recrystallized and without any precipitation has a microhardness measure at 220 HV. The dislocations present in the matrix influence the reorientation processes for superelasticity

FIG 9. A size 20 Hero 0.06 taper, maximum curved area. The defects appear very extended under strain.

(12). Both the defects and internal stresses can act as a negative factor to the mobility of martensite interfaces (8). When the annealing temperature is above 600°C the recrystallization process takes place, decreasing the density of lattice defects and internal stress produced by work-hardening (13).

SEM results show a high incidence of machining marks on the surface as more or less deep scratches. In clinical conditions the curve of canals distorts the endodontic instruments; cyclic fatigue is caused by repeated tensile-compressive stress. The maximum of this stress is in the surface of the curve. Crack nucleation and propagation stages appear mostly on the half of the instrument that is in tension (outside of the curve). The crack nucleation stage is facilitated by the high density of surface defects and then the fatigue failure is largely a crack propagation process.

CONCLUSION

Manufacture of NiTi alloys by machining in endodontic files promotes work-hardening, which defects contribute to the degradation of mechanical properties of these alloys. Cold work and heat treatments are important variables to be controlled during the manufacture of endodontic files products. In superelasticity on repeated cycling reorientation of the martensite under stress leads to gradual defect accumulation. It might be expected that these dislocations are generated at the interface between different martensite colonies. A higher dislocation density influences the reorientation processes and crack growth: the files become brittle. The phenomenon of repeated cyclic metal fatigue, caused by canal curvatures, may be the most important factor in instrument separation (14).

In these applications it is critical to predict the service life based on theoretical modeling. Some suggestions could be advanced to improve the lifetime of endodontic files:

- Apply some thermal treatments (recovery) before machining to decrease the work-hardening of the alloy
- Choose machining conditions adapted to this NiTi SMA
- An electropolishing procedure could be used by the manufacturer to reduce the machining damage on the file surface.

The authors are grateful to Dr. Luc Robbiola for SEM support and Professor Pierre Machtou for materials support.

Drs. Kuhn, Tavernier, and Jordan are affiliated with UFR d'Odontologie, Paris, France. Drs. Kuhn and Jordan are affiliated with the Laboratoire de Métallurgie Structurale, ENSCP, Paris, France. Dr. Jordan is affiliated with CECM, CNRS, Vitry sur Seine, France. Address requests for reprints to Dr. Grégoire Kuhn, Laboratoire de Métallurgie Structurale, ENSCP, 11 Rue Pierre et Marie Curie, 75231 Paris Cedex 05, France.

References

1. Walia H, Brantley WA, Gerstein H. An initial investigation of the bending and torsional properties of nitinol root canal files. J Endodon 1988;14:346–51.
2. Serene TP, Adams JD, Saxena A. Nickel-titanium instruments: applications in endodontics, St. Louis: Ishiyaku EuroAmerica, Inc., 1994.
3. Cohen S, Burns RC. Pathway of the pulp. 6th ed. St. Louis: Mosby-Year Book, Inc., 1994:206.
4. Guénin G. Alliages à mémoire de forme. Techniques de l'ingénieur 1986;10:1–11.
5. Jackson CM, Wagner HJ, Wasilewski RJ. 55-Nitinol—the alloy with a memory: its physical metallurgy, properties and application. NASA Report SP-5110, 1972:2–13.
6. Cullity BD. Element of x-ray diffraction. Chapts. 3, 4, 9, and 10. 2nd ed. Reading, MA: Addison-Wesley, 1978.
7. Miyazaki S, Ohmi Y, Otsuka K, Suzuki Y. Characteristics of deformation and transformation pseudoelasticity in NiTi alloys. J Physique 1982;43:255–60.
8. Liu Y, Van Humbeeck J, Stalmans R, Delaey L. Some aspects of the properties of NiTi shape memory alloy. J Alloys Compounds 1997;247:115–21.
9. Guinier A. Théorie et technique de la radiocristallographie. Structure des matériaux écrouis. DUNOD, 1964:560–71.
10. Melton KN, Mercier O. Fatigue of NiTi thermoelastic martensites. Acta Metall 1979;27:137–44.
11. Treppmann D, Hornbogen E, Wurzel LD. The effect of combined recrystallization and precipitation process on the functional and structural properties in NiTi alloys. J Physique IV 1995;5:569–74.
12. Filip P, Mazanec K. Influence of cycling on the reversible martensitic transformation and shape memory phenomena in NiTi alloys. Scripta Metall Mater 1994;30:67–72.
13. Liu Y, McCormick PG. Proc. ICOMAT-92, Monterey Inst. for Advanced Studies, 1993:923.
14. Sotokawa T. An analysis of clinical breakage of root canal instruments. J Endodon 1988;14:75–82.

The *Journal of Endodontics'* "Ask A Friend" feature provides a forum for subscribers to submit a clinical case about which they have questions and have it published in the *Journal*, along with a review by one of a panel of "Friends." The person submitting the case may remain anonymous upon request. To learn of the procedures for submitting an article, check the January 1998 issue of the *Journal*.